ChemComm

COMMUNICATION

View Article Online
View Journal | View Issue

Cite this: *Chem. Commun.*, 2020, **56**, 5743

Received 4th March 2020,
Accepted 30th March 2020

DOI: 10.1039/d0cc01686a

rsc.li/chemcomm

Photoreforming of biomass in metal salt hydrate solutions†‡

Christian M. Pichler, Taylor Uekert and Erwin Reisner *

Metal salt hydrate (MSH) solutions allow for the complete solubilisation of biomass and we demonstrate its use as a reaction medium for the photocatalytic reforming of lignocellulose. Different types of photocatalysts such as TiO_2 and carbon nitride can be employed in MSH to produce H_2 and organic products under more benign conditions than the commonly required extreme pH aqueous solutions.

Photoreforming (PR) allows for the simultaneous production of H_2 gas and organic products from the sunlight-driven conversion of waste polymeric substrates such as biomass and plastics in aqueous medium under ambient temperature and pressure.[1–6] TiO_2 is the archetypical photocatalyst for this process, and CdS quantum dots and carbon nitride (CN_x) have recently been reported as visible-light absorbing alternatives.[7–11]

Efficient PR requires the substrate to easily access the photocatalyst, which poses a challenge for an insoluble polymeric substrate in combination with a heterogeneous photocatalyst.[4,12] Lignocellulose is a highly desirable substrate for the PR process due to its abundance as inedible biomass waste and potentially interesting reaction products.[13] However, its recalcitrance demands harsh reaction conditions such as extremely alkaline or acidic media for complete solubilisation.

Employing PR under more benign conditions has the potential to improve the sustainability and efficiency of the process. Lignocellulosic biomass can be solubilised at relatively mild conditions in metal salt hydrate (MSH) solutions.[14–16] Very high concentrations of inorganic salts such as LiBr with low acid concentrations in water can be used to depolymerise lignocellulosic biomass into soluble sugars.[17–19] Li^+ coordinates water molecules strongly and thereby generates acidity that aids cellulose depolymerisation. The presence of Br^- exhibits favourable hydrogen bonding interactions with the cellulose chain.[14,19] The majority of studies in MSH have so far solely focussed on the dissolution process of cellulose. Investigations into the chemical conversion of depolymerised cellulose in MSH solutions are rare,[20,21] and PR in MSH solutions has not yet been explored.

Here, we report PR of cellulose and real-world lignocellulosic biomass in MSH solutions for the co-production of H_2 gas and soluble organic products (Fig. 1). We show the depolymerisation of cellulosic substrates in LiBr MSH solutions, followed by PR of the solubilised sugars with photocatalyst suspension systems based on different TiO_2 and CN_x particles. The influence of LiBr concentration and pH value on PR performance is also investigated.

First, the dissolution of microcrystalline cellulose (100 mg) in a LiBr MSH solution (2 mL of 62.5 wt% LiBr in aqueous 0.1 M H_2SO_4) at 90 °C open to air was studied. The cellulose was completely dissolved after 30 min and the dissolved products were analysed by high performance liquid chromatography (HPLC) after

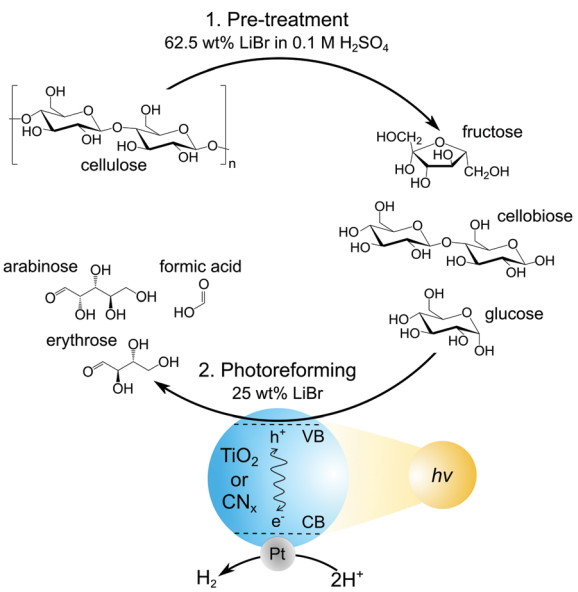

Fig. 1 Schematic overview of the PR process in MSH solution.

Department of Chemistry, University of Cambridge, Lensfield Road, Cambridge CB2 1EW, UK. E-mail: reisner@ch.cam.ac.uk; Web: http://www-reisner.ch.cam.ac.uk

† Data related to this publication are available at the University of Cambridge data repository: https://doi.org/10.17863/CAM.51141.

‡ Electronic supplementary information (ESI) available. See DOI: 10.1039/d0cc01686a

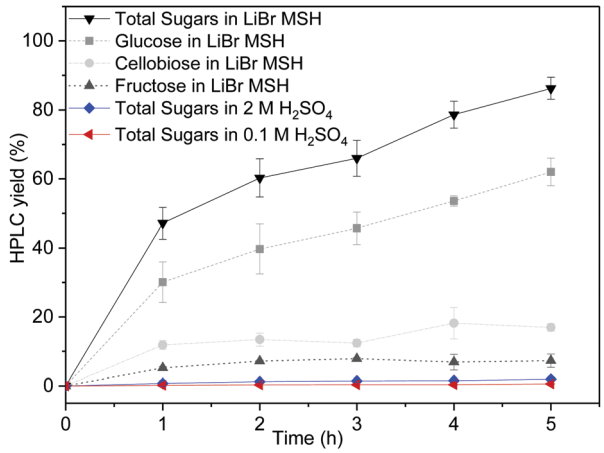

Fig. 2 Yield of soluble products from dissolution of microcrystalline cellulose (100 mg) in 2 mL LiBr MSH (62.5 wt% LiBr in 0.1 M H_2SO_4), 0.1 M H_2SO_4 (no LiBr) and 2 M H_2SO_4 (no LiBr) at 90 °C. The yield of total sugars is the sum of glucose, fructose and cellobiose. Error bars indicate standard deviation.

regular time intervals. Gradual depolymerisation of the cellulose chains into low molecular sugars is observed, with more than 90% of cellulose being converted into glucose, cellobiose and fructose after 5 h (Fig. 2). The concentration of cellobiose remains at approximately 20% in the course of the hydrolysis reaction and fructose results from acid-catalysed isomerisation of glucose.

For comparison, dissolution of cellulose in aqueous 0.1 M and 2 M H_2SO_4 without LiBr was also studied under the otherwise same experimental conditions (90 °C). The cellulose remains mostly insoluble in the absence of LiBr-based MSH. Only minor amounts of dissolved sugars are formed by the depolymerisation of the cellulose chains: ~2% total molecular sugars in 2 M H_2SO_4 and <1% in 0.1 M H_2SO_4. The LiBr MSH is therefore crucial for effective cellulose dissolution and depolymerisation.

The cellulose solutions after 5 h MSH treatment were subsequently used for PR with a variety of photocatalyst particles. The photocatalysts were prepared by loading 1 wt% Pt onto different types of TiO_2 (P25, anatase and rutile) nanoparticles and cyanamide-functionalised carbon nitride ($^{NCN}CN_x$) powder (see ESI‡ for experimental procedures and materials characterisation and Fig. S1 and S2, Pt particle size 5–15 nm for TiO_2 supports and 3–8 nm for $^{NCN}CN_x$).[2,3,22] The latter was employed due to its visible light absorbing properties and high activity to oxidise alcohols, including sugars, over its cyanamide functionality.[7,8,23–25]

To prepare the standard PR solution, 1 mL of the cellulose lysate in LiBr MSH solution (62.5 wt% LiBr in 0.1 M H_2SO_4) was added to 1.5 mL H_2O containing 4 mg dispersed photocatalyst (final LiBr concentration: 25 wt%; see Fig. 1). This solution was then used for PR under simulated solar light irradiation (AM1.5G at 100 mW cm^{-2}) for 24 h at 25 °C. The amount of H_2 produced from PR was quantified by gas chromatography and the oxidation products by HPLC (dilution of reaction solution 10 : 1 with H_2O for analysis, Fig. 3). PR activities in MSH-free solutions using aqueous H_2SO_4 (2 M) are also shown for comparison. In this case cellulose was pre-treated for 5 h at 90 °C in 2 M H_2SO_4, where only 2% of cellulose are converted into soluble sugars (Fig. 2). 1 mL of this solution was diluted with 1.5 mL H_2O and subjected to PR.

The three TiO_2 photocatalysts show a far higher rate of H_2 production in LiBr MSH treated cellulose compared to a control experiment in 2 M H_2SO_4. This result demonstrates the benefit of dissolution and depolymerisation of cellulose in LiBr MSH solution and the compatibility with the PR process. The lower available amount of soluble sugars from the H_2SO_4 treatment results in a lower H_2 yield. The formation rates of oxidation products in Fig. 3 for rutile are twice than for P25 and anatase nanoparticles, although the difference in H_2 yield is only around 20%. This may be explained by the different reaction mechanisms of the catalysts,[26] as rutile forms surface bound

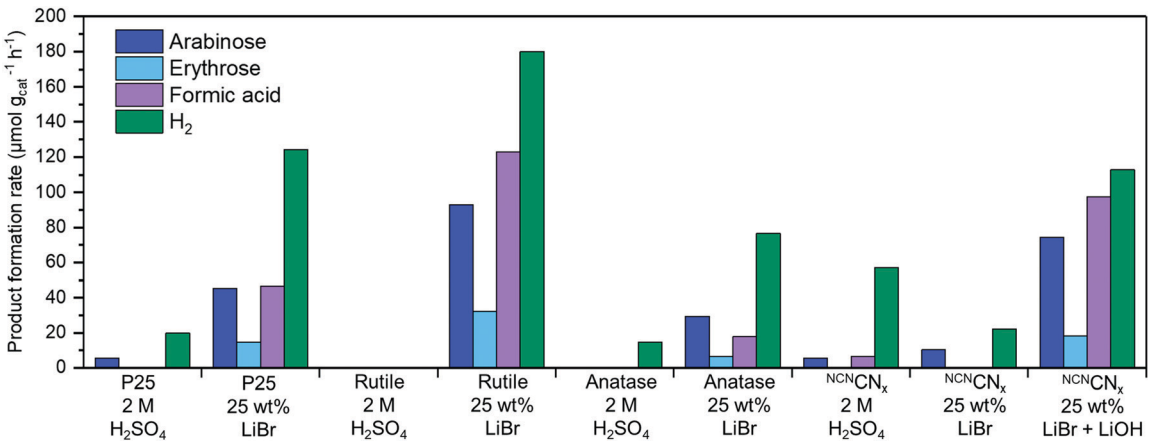

Fig. 3 Photoreforming results after 24 h using different photocatalysts and conditions using AM 1.5G, 100 mW cm^{-2} irradiation at 25 °C. Cellulose (50 mg) in 1 mL of 62.5 wt% LiBr in 0.1 M H_2SO_4 is added to 1.5 mL aqueous solution containing 4 mg photocatalyst to give 2.5 mL of 25 wt% LiBr. Note that organic products originating from alkaline degradation in the dark were subtracted from the values obtained during PR with $^{NCN}CN_x$ in 25 wt% LiBr with LiOH (see ESI‡ for details). Standard deviations for H_2 yields can be found in Table S1 (ESI‡) (between 5–20%). Taking these deviations and the error for the HPLC analysis into account, standard deviation for the organic products can be estimated to be around 20%.

radicals and P25/anatase free OH radicals.[26] This was confirmed by determining the yield of hydroxy radicals using fluorescence studies in H_2O and 25 wt% LiBr solutions (ESI,‡ Fig. S3).[27]

The $^{NCN}CN_x$ photocatalyst shows low activities in both conditions, which can be explained by the acid hydrolysis of cyanamide in $^{NCN}CN_x$ (bleaching of the material becomes visibly apparent over time).[23,28,29] The hydrolysis of the cyanamide was confirmed by infrared spectroscopy that shows the decline of the characteristic cyanamide peak at 2180 cm^{-1} under the standard PR conditions (ESI,‡ Fig. S4).

Despite degradation and lower activity under standard conditions, the $^{NCN}CN_x$ photocatalyst has the benefit of visible light absorption.[8] PR experiments using cellulose in 25 wt% LiBr with a UV filter ($\lambda > 400$ nm irradiation) produces 3.1 μmol g_{cat}^{-1} h^{-1} H_2 with $^{NCN}CN_x$ (ESI,‡ Table S1, entry 16). The wide-band gap semiconductor TiO_2 did not show any activity with UV-filtered light,[30] which is consistent with the previously reported absence of visible light absorbing charge-transfer complexes with TiO_2 and glucose.[31]

To prevent degradation of $^{NCN}CN_x$, we have also explored basic conditions for PR and added 1 mL cellulose LiBr (62.5 wt%) MSH containing 0.1 M H_2SO_4 into 1.5 mL of aqueous 0.1 M LiOH instead of pure H_2O. The alkaline medium does not significantly hydrolyse the cyanamide-functionality,[7,8] and enhances the PR performance of the $^{NCN}CN_x$ photocatalyst substantially (giving 112 μmol H_2 g_{cat}^{-1} h^{-1} and also higher yields of organic products). Visible light only irradiation ($\lambda > 400$ nm) produced 49 μmol H_2 g_{cat}^{-1} h^{-1} and organic oxidation products (ESI,‡ Table S1, entry 17). In a control PR experiment with cellulose in 0.1 M LiOH without LiBr MSH only minor amounts of H_2 (0.8 μmol g^{-1} h^{-1}) and no organic reaction products were generated (ESI,‡ Table S1, entry 15). When the alkaline conditions (LiBr MSH + 0.1 M LiOH) are used for the rutile photocatalyst, the H_2 production rate drops from 180 μmol H_2 g_{cat}^{-1} h^{-1} (25 wt% LiBr) to 16 μmol H_2 g_{cat}^{-1} h^{-1} (25 wt% LiBr + 0.1 M LiOH), together with the yield of organic oxidation products (ESI,‡ Table S1, entry 9). The decreased photocatalytic activity of TiO_2 in alkaline pH is consistent with previous reports.[32]

Next, PR using a real-world lignocellulose substrate was explored. Beech-wood sawdust was treated with LiBr MSH and the wood-lysate was used under standard PR conditions for 96 h with rutile (the best preforming TiO_2 photocatalyst for cellulose) and $^{NCN}CN_x$ (+LiOH) under UV-vis irradiation (ESI,‡ Fig. S5). The MSH depolymerised and dissolved the cellulosic part of wood, while lignin remained undissolved and was filtered off before the start of the PR process. When beech-wood is used, the H_2 yield (1.2 μmol H_2 in 24 h for $^{NCN}CN_x$ and 0.5 μmol H_2 in 24 h for rutile) as well as the yield of organic products (0.8 μmol arabinose and 1.6 μmol erythrose in 24 h for $^{NCN}CN_x$ as well as 2.4 μmol arabinose and 1.0 μmol erythrose in 24 h for rutile) is lower compared to pure cellulose as substrate, which may be due to reduced light transmission through the brown-coloured wood degradation products in the solution.

Finally, we investigated the role of LiBr in the PR process using glucose as a model substrate.[33] PR of glucose in water was compared with PR under standard conditions (1 mL of the 62.5 wt% LiBr, 0.1 M H_2SO_4 solution is added to 1.5 mL H_2O; final concentration 25 wt% LiBr) using P25, rutile, anatase or $^{NCN}CN_x$ as catalyst. In pure H_2O, $^{NCN}CN_x$ is the most active catalyst followed by rutile TiO_2 (ESI,‡ Fig. S6). The presence of LiBr under standard conditions changes the relative PR performance substantially: the activity of all three TiO_2 catalysts is reduced by 50–70%, (P25 from 327 to 129, rutile from 436 to 226 and anatase from 322 to 112 μmol H_2 g_{cat}^{-1} h^{-1}), whereas the H_2 yield for $^{NCN}CN_x$ is decreased by more than 95% (from 672 to 24 μmol H_2 g_{cat}^{-1} h^{-1}). Under these conditions, rutile is the most active catalyst. When the MSH concentration is gradually increased from 2.5 to 25% LiBr (including corresponding amounts of H_2SO_4) (ESI,‡ Fig. S7) an abrupt decline of activity is observed for $^{NCN}CN_x$ by losing approximately two thirds of its activity already at 2.5 wt% LiBr (672 to 204 μmol H_2 g_{cat}^{-1} h^{-1}), whereas the decline for P25 is slower and more gradual (327 μmol H_2 g_{cat}^{-1} h^{-1} in pure H_2O and 324 μmol H_2 g_{cat}^{-1} h^{-1} at 2.5 wt% LiBr). The reduction in PR activity is consistent with a decrease in adsorption of glucose on the photocatalyst in the presence of LiBr (ESI,‡ Fig. S6 and S7). It is thus likely that the adsorption of LiBr ions on the heterogeneous catalyst surface blocks adsorption sites for glucose and hinders its photooxidation.[34]

In conclusion, we demonstrate that MSH solutions are a suitable medium for PR of lignocellulosic biomass. Using MSH offers the advantage of depolymerising cellulose under comparably mild conditions to soluble sugars, which can readily access the colloidal photocatalyst during the PR process to produce H_2 as well as arabinose, erythrose and formic acid. Real-world lignocellulosic wood biomass is a suitable substrate for PR in MSH solutions. Our results also show that the presence of high LiBr concentrations reduces the catalytic activity of the photocatalysts, but this deactivation is far outweighed by the drastic enhancement of solubilisation and depolymerisation of polymeric cellulose in biomass PR. We therefore envision that further improvements in biomass PR can be achieved in the future with photocatalysts that do not suffer from partial deactivation from MSH adsorption.

Support from the Austrian Science Fund (FWF; Erwin Schrödinger Fellowship J-4381 to C. M. P.), EPSRC (nanoDTC, EP/L015978/1 and EP/S022953 to T. U. and E. R.) and OMV (E. R.) is gratefully acknowledged. We also thank Dr Heather Greer for support with electron microscopy and Dr Ana Belenguer for help with HPLC. Dr Tengfei Li and Mr Arjun Vijeta are acknowledged for helpful comments and discussions.

Conflicts of interest

There are no conflicts to declare.

Notes and references

1 M. F. Kuehnel and E. Reisner, *Angew. Chem., Int. Ed.*, 2018, **57**, 3290–3296.
2 A. V. Puga, *Coord. Chem. Rev.*, 2016, **315**, 1–66.
3 G. Zhang, C. Ni, X. Huang, A. Welgamage, L. A. Lawton, P. K. J. Robertson and J. T. S. Irvine, *Chem. Commun.*, 2016, **52**, 1673–1676.
4 T. Uekert, M. F. Kuehnel, D. W. Wakerley and E. Reisner, *Energy Environ. Sci.*, 2018, **11**, 2853–2857.
5 T. Kawai and T. Sakata, *Nature*, 1980, **286**, 474–476.

6 Q. Xu, Y. Ma, J. Zhang, X. Wang, Z. Feng and C. Li, *J. Catal.*, 2011, **278**, 329–335.
7 H. Kasap, D. S. Achilleos, A. Huang and E. Reisner, *J. Am. Chem. Soc.*, 2018, **140**, 11604–11607.
8 T. Uekert, H. Kasap and E. Reisner, *J. Am. Chem. Soc.*, 2019, **141**, 15201–15210.
9 A. Speltini, M. Sturini, D. Dondi, E. Annovazzi, F. Maraschi, V. Caratto, A. Profumo and A. Buttafava, *Photochem. Photobiol. Sci.*, 2014, **13**, 1410–1419.
10 H. Hao, L. Zhang, W. Wang and S. Zeng, *ChemSusChem*, 2018, **11**, 2810–2817.
11 D. W. Wakerley, M. F. Kuehnel, K. L. Orchard, K. H. Ly, T. E. Rosser and E. Reisner, *Nat. Energy*, 2017, **2**, 17021.
12 X. Wu, X. Fan, S. Xie, J. Lin, J. Cheng, Q. Zhang, L. Chen and Y. Wang, *Nat. Catal.*, 2018, **1**, 772–780.
13 X. Liu, X. Duan, W. Wei, S. Wang and B. J. Ni, *Green Chem.*, 2019, **21**, 4266–4289.
14 N. Rodriguez Quiroz, A. M. Norton, H. Nguyen, E. Vasileiadou and D. G. Vlachos, *ACS Catal.*, 2019, **9**, 9923–9952.
15 S. Fischer, H. Leipner, K. Thümmler, E. Brendler and J. Peters, *Cellulose*, 2003, **10**, 227–236.
16 S. Sen, J. D. Martin and D. S. Argyropoulos, *ACS Sustainable Chem. Eng.*, 2013, **1**, 858–870.
17 W. Deng, J. R. Kennedy, G. Tsilomelekis, W. Zheng and V. Nikolakis, *Ind. Eng. Chem. Res.*, 2015, **54**, 5226–5236.
18 R. M. de Almeida, J. Li, C. Nederlof, P. O'Connor, M. Makkee and J. A. Moulijn, *ChemSusChem*, 2010, **3**, 325–328.
19 N. Rodriguez Quiroz, A. M. D. Padmanathan, S. H. Mushrif and D. G. Vlachos, *ACS Catal.*, 2019, **9**, 10551–10561.
20 C. G. Yoo, S. Zhang and X. Pan, *RSC Adv.*, 2017, **7**, 300–308.
21 S. Sadula, O. Oesterling, A. Nardone, B. Dinkelacker and B. Saha, *Green Chem.*, 2017, **19**, 3888–3898.
22 X. Zhou, Y. Li, Y. Xing, J. Li and X. Jiang, *Dalton Trans.*, 2019, **48**, 15068–15073.
23 V. W. H. Lau, I. Moudrakovski, T. Botari, S. Weinberger, M. B. Mesch, V. Duppel, J. Senker, V. Blum and B. V. Lotsch, *Nat. Commun.*, 2016, **7**, 12165.
24 H. Kasap, C. A. Caputo, B. C. M. Martindale, R. Godin, V. W. H. Lau, B. V. Lotsch, J. R. Durrant and E. Reisner, *J. Am. Chem. Soc.*, 2016, **138**, 9183–9192.
25 A. Sattler and W. Schnick, *Eur. J. Inorg. Chem.*, 2009, 4972–4981.
26 R. Chong, J. Li, Y. Ma, B. Zhang, H. Han and C. Li, *J. Catal.*, 2014, **314**, 101–108.
27 S. Nagarajan, N. C. Skillen, F. Fina, G. Zhang, C. Randorn, L. A. Lawton, J. T. S. Irvine and P. K. J. Robertson, *J. Photochem. Photobiol., A*, 2017, **334**, 13–19.
28 V. W. H. Lau, V. W. Z. Yu, F. Ehrat, T. Botari, I. Moudrakovski, T. Simon, V. Duppel, E. Medina, J. K. Stolarczyk, J. Feldmann, V. Blum and B. V. Lotsch, *Adv. Energy Mater.*, 2017, **7**, 1602251.
29 A. Vijeta and E. Reisner, *Chem. Commun.*, 2019, **55**, 14007–14010.
30 R. Beranek, *Adv. Phys. Chem.*, 2011, 80–83.
31 G. Kim, S. Lee and W. Choi, *Appl. Catal., B*, 2015, **162**, 463–469.
32 X. Fu, J. Long, X. Wang, D. Y. C. Leung, Z. Ding, L. Wu, Z. Zhang, Z. Li and X. Fu, *Int. J. Hydrogen Energy*, 2008, **33**, 6484–6491.
33 L. Da Vià, C. Recchi, E. O. Gonzalez-Yañez, T. E. Davies and J. A. Lopez-Sanchez, *Appl. Catal., B*, 2017, **202**, 281–288.
34 C. Guillard, E. Puzenat, H. Lachheb, A. Houas and J. M. Herrmann, *Int. J. Photoenergy*, 2005, **7**, 641208.